Petrology, Vol. 11, No. 4, 2003, pp. 327–342. Translated from Petrologiya, Vol. 11, No. 4, 2003, pp. 363–380.

Geochemical Classification of Silicic Igneous Rocks of Major Geodynamic Environments

S. D. Velikoslavinskii

Institute of Precambrian Geology and Geochronology, Russian Academy of Sciences, nab. Makarova 2, St. Petersburg, 199034 Russia
e-mail: SDTJ@SV1403.spb.edu

Received October 26, 2001

Abstract—A large body of published geochemical data on the Phanerozoic granitoids of within-plate, collision, and subduction environments was used to revise the universally accepted methods for the determination of the geodynamic setting of granitoid formation on the basis of chemical characteristics. Possible errors related to the use of particular methods were distinguished. The granitoids of the environments considered were geochemically characterized and the conclusion on their geochemical individuality was confirmed. On the basis of the discriminant analysis of available geochemical data, a set of discriminant functions was calculated for improved analytical or graphical solution of the problem of the tectonic correlation of granitoids of primary magmatic nature (volcanics of dacite–rhyolite composition and intrusive granitoids and granites containing more than 65 wt % SiO_2) using the concentrations of either major elements only or major and trace elements. The proposed discriminant functions were tested on the example of Precambrian granitoids, which illustrated prospects of their use for the tectonic reconstructions of Precambrian regions.

INTRODUCTION

A number of studies demonstrated that igneous rocks, including silicic ones, formed in different geodynamic environments show significantly different chemical compositions. This fact provides a basis for the use of geochemical rock characteristics in paleotectonic reconstructions. The methods that are now used for the discrimination of silicic igneous rocks of various settings on the basis of their chemical compositions were proposed 10–15 years ago and are not free of drawbacks. In particular, many of them were constructed using limited input data, and the mathematical methods of data processing were also not optimal.

The importance of the determination of the tectonic position of granitoids from their geochemical characteristics is beyond doubt. It is of special importance for the tectonic analysis of the Early Precambrian, where other (in particular, geological) methods of geodynamic correlation are often impracticable. Because of this, it is necessary to assess on the basis of a more representative data set, which was compiled through the generalization of a large body of analytical data accumulated up to now in the geological literature, the efficiency of previously proposed methods. Furthermore, if they will appear to be inadequate, new geochemical criteria must be developed for the classification of granitoids of major geodynamic settings, which are more consistent with the available data. There is a vast body of analytical data in the literature on diverse granitoids represented by the results of silicate analysis only. Since the most widely used methods are based on trace-element data, it is of special interest to construct criteria for the geochemical classification of granitoids using analytical results for both trace and major elements. Taking into account these considerations, the following problems were addressed in our study:

(1) assessment of available geochemical methods for the tectonic classification of granitoids;

(2) estimation of the generalized geochemical characteristics of granitoids of major geodynamic environments;

(3) development of multidimensional geochemical criteria for the tectonic classification of granitoids on the basis of both silicate analyses and the optimum set of trace elements; and

(4) testing of the proposed criteria on the example of some Precambrian granitoids.

INITIAL DATA

The problems formulated can be obviously solved only on the basis of generalization of analytical data for granitoids published in the geological literature. In this paper we considered the available data that were used for the construction of traditional discriminant diagrams (Pearce *et al.*, 1984; Papu *et al.*, 1989; Thïblemont and Cabanis, 1990) and those used by Förster *et al.* (1997) for the evaluation of the (Y + Nb)–Rb diagram. In addition, the input data set was significantly expanded at the expense of a large volume of geochemical information on granitoids from the territory of Russia and the former USSR and data from recent publications.

This paper is concerned with the geochemical characteristics of silicic igneous rocks of subduction,

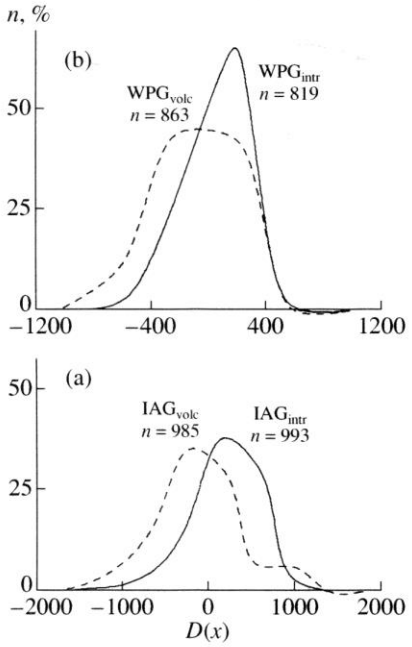

Fig. 1. Results of the discriminant analysis of intrusive granitoids and volcanics from (a) subduction and (b) collisional settings. *n*, % is the volume of the data set.

within-plate, and collision settings. In contrast to previous work (Pearce *et al.*, 1984; Papu *et al.*, 1989; Thïblemont and Cabanis, 1990), the granitoids of mid-ocean ridge and suprasubduction environments were not considered, because these settings are more efficiently recognized using the geochemical characteristics of mafic and ultramafic rocks.

It is worth noting that the well-known diagrams for the discrimination of granitoids of main geodynamic settings by chemical characteristics were constructed using the data on both intrusive and volcanic rocks, although the validity of such an approach was never specially investigated. The discriminant analysis of intrusive granitoids and silicic volcanics from subduction and within-plate settings (Fig. 1) demonstrated that their chemical compositions are identical, which allows us to use with more confidence a combined data set on intrusive and volcanic rocks for the evaluation of geochemical characteristics of the silicic magmatism of major geodynamic settings. Thus, the assembled initial data reflect the chemical composition of silicic igneous rocks as a whole. Because of this, the groups of igneous rocks considered are collectively referred to as granitoids.

Igneous rocks from island-arc environments are statistically represented by continuous differentiated series from basic to silicic rocks. The maximum of the distribution varies depending on the type of an island arc. Igneous rocks from within-plate environments are represented with rare exceptions by bimodal associations with distribution maxima at gabbro and granite compositions. The statistically felsic component of the bimodal association corresponds to rocks with SiO_2 > 65 wt %. Granites are the most abundant rocks in collision environments, and more basic rocks occur in minor amounts. In this respect, the correct comparison of the chemistry of granitoids from various geodynamic settings requires a selection of common intervals of differentiated series, for instance, intervals with identical SiO_2 contents. This condition is met, if granitoids with SiO_2 > 65 wt % are considered, which is done below.

The results of the silicate analysis of granitoids are often reported on a water-free basis. Because of this, all petrochemical data were also recalculated to water-free compositions.

The general characteristics of granitoids from the geodynamic environments considered whose geochemical data were used for further investigations are given in Table 1.

The complete list of the sources of initial data includes more than 400 references and could not be published in this paper. However, if necessary, all the information on data sources is available from the author via e-mail (SDTJ@SV1403.SPB.EDU).

The compiled analytical information is not the full inventory of geochemical data for granitoids formed in the geodynamic settings under consideration. However, the wide regional and age scatter of available data suggests that they are representative with respect to geodynamic settings and excludes the possibility of interpretation of the chemical features of the granitoids as a result of the manifestation of regional or time evolution differences. The total volume of analytical data is characterized in Table 2.

Before proceeding with the geochemical characteristics of the granitoid groups considered, it is necessary to address the problem of comparison of different analytical data. It is commonly believed that the results of silicate analyses obtained in different laboratories are adequately compatible with each other, whereas the results of the determination of trace elements obtained by various methods in various laboratories may differ significantly. Probable exceptions are the results of determination of rare earth elements (REE) and Rb and Sr isotopic data. Owing to high analytical precision, the systematic errors of various laboratories and methods and random errors are probably relatively low for these parameters. In fact, the problem of reduction of diverse analytical data to the form of equal accuracy and precision has no solution even if the metrological parameters of analytical methods are known. Because of this, there are only two variants: one can either use different analytical data in the form in that they were published ignoring analytical errors or do not use them at all. Fortunately, there is some indirect evidence allowing us to accept the former variant. For instance, each of the granitoid groups considered was characterized to the

Table 1. Generalized characteristics of granitoid complexes used in this work (numbers of silicate analyses are shown in parentheses)

Geodynamic setting			Region, complex, pluton
Subduction	Modern island arcs	oceanic	Granitoids of Mariana and Tonga–Kermadec–New Zeeland arcs (27)
		developed	Granitoids of the Aleutian–Alaskan (144), Kurile–Kamchatka (436), Fiji (12), and New Hebrides (3) arcs
		mature	Granitoids of the Japan (152), New Guinea (63), Indonesia (12), and Mediterranean (66) arcs; Lesser Antilles (29); and others (37)
	Continental arcs and continental margins		Granitoids of the Mesozoic–Cenozoic belts of the Pacific margin of North America (330), Pacific margin of South America (185), northwestern Pacific margin of Russia (35), and continental margins of other regions (45)
	Phanerozoic paleoarcs		Granitoids of the paleoarcs of the Caucasus, Urals, Blue Mountain, West Shasta, and others (229)
Collisional	Syncollisional		1. Early Paleozoic granitoids related to the collision of the West African craton and the Tuareg shield: Iforas batholith (36) 2. Granitoids of the Hercynian collision zones of western Europe: Trois Seigneurs pluton, Pyrenees; Pedrobernardo, Spain; Braga and Lixa, northern Portugal; Boodmin, Dartmoor, St. Austell, Brannel, Carmenell, Meldon, Lands End, and Cornubian, England; Moldanubian, Austria; Velay complex, Massif Central, France; and others (307) 3. Paleozoic granitoids of collisional zones of the Atlantic margin of North America: plutons of the Meguma zone, Nova Scotia; plutons of the Gander zone, Brunswick; Ackley City batholith, Newfoundland; and others (144) 4. Granitoids of the India–Asia collision zone: Manaslu complex, Gangotori leucogranite plutons, Karakorum (Himalaya), and others (177); and Guntskii complex, Pamirs (29) 5. Mesozoic granitoids of various collision zones of the Pacific margin of Russia: Grodekovskii and Khungariiskii complexes (50)
	Late-collisional		1. Granitoids of the Hercynian collision zones of western Europe: Sardinia–Corsica batholith, plutons of the Iberian massif, Querigut pluton (Pyrenees), Central Bohemian pluton (Czech Republic), Southern Bohemian pluton (Austria), Eisgarn, Fichtelgebirge, Erzgebirge, Falkenberger, and Steinwald plutons, Germany; and others (480) 2. Granitoids of the India–Asia collision zone: Lhasa and other plutons of the Himalaya; Bazarryk-skii, Ortobuzskii, Bashgumbezskii, and Bazardarinskii complexes, Pamirs; and others (285)
	Syncollisional and late-collisional undifferentiated		1. Proterozoic and Paleozoic granitoids related to the collision of the Kara microcontinent and the Siberian craton, Taimyr (21) 2. Granitoids related to the Early Mesozoic collision of the Kolyma microcontinent and the Verkhoyansk continental margin of the Siberian craton: Nelkanskii, Nelchenskii, Nyurgun-Tasskii, Chimgalinskii, Ust'-Nera, Kigilyakhskii, Chalbinskii, Chimgalinskii, Kere-Yuryakh, and other massifs (211) 3. Hercynian granitoids of the tin-bearing belt of southeastern Asia related to the accretion of Laurasia, Thailand (152) 4. Mesozoic granitoids of the collision zones of the Pacific margin of North America: White Creek batholith; plutons of the Kootenay arc, Canadian Cordillera; Hall Canyon pluton, California; and others (81) 5. Granitoids of various ages of the southwestern framing of the Siberian platform (42) 6. Mesozoic granitoids of various collision zones of the Pacific margin of Russia, Sandinskii complex (5) 7. Granitoids of various regions: Caucasus, Urals, New Zeeland, Carpathians, and others (67)
Within-plate	Oceanic		Volcanic and intrusive complexes of the islands of Galapagos, Guadeloupe, Iceland, and Ascension (54)
	Continental		1. Granitoids of ring complexes: Nigeria, Sudan, Arabian shield, North Wales, Corsica, and other regions (300) 2. Granitoids of modern and paleocontinental rifts: Afar, Kenya, Ethiopia, California, Mexico, Central Asia, Oslo, and other rift zones (636) 3. Granitoids of continental flood basalt provinces: Brazil, Deccan, Karoo, northwest Scotland, Yellowstone Plateau, Campbell Island, and others (201) 4. Granitoids of settings transitional from back-arc spreading to continental rifting: Trans-Pecos province, Latir, Henderson, and New Zeeland (296) 5. Proterozoic anorogenic granitoids including rapakivi granites: Ulkanskii and Korosten plutons, plutons of Brazil and Australia (255) 6. Granitoids of undifferentiated within-plate settings (69)

Table 2. Average chemical compositions of granitoids ($SiO_2 > 65$ wt %) of major geotectonic environments

Component	Subduction granitoids						Collisional granitoids						Within-plate granitoids					
	X	S	M	Q_L	Q_H	n	X	S	M	Q_L	Q_H	n	X	S	M	Q_L	Q_H	n
SiO_2	70.62	3.52	70.27	67.72	73.42	1805	72.62	2.63	73.02	70.82	74.47	2027	74.1	2.74	74.69	72.42	76.24	1811
TiO_2	0.42	0.2	0.41	0.27	0.55	1805	0.29	0.18	0.27	0.14	0.42	2027	0.26	0.19	0.22	0.12	0.36	1811
Al_2O_3	15.04	1.38	15.16	14.11	16	1805	14.69	1.03	14.76	14.04	15.3	2027	12.79	1.47	12.82	12.07	13.6	1811
FeO	3.12	1.33	3.11	2.12	4.02	1805	2.06	1.05	1.95	1.29	2.76	2027	2.79	1.63	2.48	1.51	3.74	1811
MnO	0.08	0.06	0.07	0.05	0.1	1805	0.05	0.04	0.05	0.03	0.06	2027	0.07	0.07	0.05	0.03	0.09	1811
MgO	1.04	0.65	0.93	0.51	1.47	1805	0.62	0.52	0.48	0.2	0.9	2027	0.2	0.2	0.12	0.05	0.28	1811
CaO	3	1.35	3.02	1.97	4.05	1805	1.41	0.89	1.19	0.73	1.91	2027	0.68	0.55	0.51	0.28	0.91	1811
Na_2O	4.11	0.72	4.09	3.64	4.63	1805	3.47	0.51	3.43	3.14	3.76	2027	4.28	0.98	4.15	3.61	4.86	1811
K_2O	2.48	1.28	2.4	1.45	3.4	1805	4.53	0.77	4.53	4.04	5.03	2027	4.75	0.65	4.71	4.37	5.14	1811
P_2O_5	0.12	0.07	0.1	0.06	0.16	1572	0.21	0.14	0.18	0.1	0.28	1818	0.06	0.07	0.03	0.01	0.07	1501
Ba	700	507	642	407.5	859.5	975	418	382	325	132	625	1150	328	405	120	35	554	1134
Sr	336	227	284	166	450	1045	158	170	97	55	193	1241	60	79	58.9	10	83.4	1270
Rb	75	52	67	32.5	104.5	1032	401	456	282	188	409	1286	292	254	209	143	342	1382
Nb	8.2	5.7	7.5	4.95	11	687	22.1	19.9	17	12	23.2	911	110.2	159.8	70	31.5	130	1210
Zr	154	81	141	99	197	934	125	73	120	66	172	998	608	778	356	164	789.5	1287
Hf	4.69	2.35	4.17	3.1	6	451	3.63	1.85	3.48	2.2	4.78	395	15.64	19.02	10.73	6.3	18	478
Ta	0.89	1.46	0.55	0.36	0.96	354	4.56	4.41	3	1.62	6	527	11.09	25.5	5.5	3.1	9.4	441
Th	10	10.41	8	3.4	13.3	663	20.78	17.1	18	9	29	759	35.4	37.2	26.8	18.2	41	746
U	2.6	2.2	2	1.25	3	435	11.4	8.2	9	5	15	596	8.7	9.6	6.2	4	10.7	526
Ga	16.2	3.5	16.2	14	18	159	21.3	6.3	20	17	24	477	33.7	11.9	32	25	40	292
La	22.2	16.2	20	13	28.5	694	32.4	24.4	30	15	43.1	809	83	64.1	69	43	110	818
Ce	42.2	27	38.65	26	52	696	63.1	42.4	60.2	30	86.3	833	154.7	114.8	132	82.2	201.5	859
Pr	4.1	2.6	3.8	2.2	5.9	118	7	5.8	6.5	3.8	9.8	244	25.8	20.1	21	15	25	107
Nd	18.8	9.7	17.6	12.4	23.6	588	25.6	18.9	25	11.2	34	675	68.3	55.1	57.7	32.2	88.7	676
Sm	4.3	2.3	4	2.7	5.4	540	5.4	4.4	5	2.8	6.9	650	13.7	11.3	11.8	6.6	17.5	600
Eu	0.96	0.46	0.88	0.67	1.16	538	0.69	0.8	0.6	0.3	0.98	541	1.06	1.01	0.76	0.22	1.66	623
Gd	3.87	2.06	3.7	2.4	4.85	299	4.19	2.73	3.93	2.16	5.61	342	13.9	11.39	12.45	6.5	17	322
Tb	0.67	0.46	0.6	0.4	0.86	448	0.68	0.65	0.57	0.36	0.77	374	2.43	1.85	2.04	1.24	3.12	465
Dy	3.16	1.98	2.7	1.71	4.34	146	4.26	4.01	3.31	1.98	4.93	265	15.16	20.46	9.76	5.51	16.5	184
Ho	0.74	0.48	0.68	0.37	1.07	111	0.93	1.08	0.56	0.33	0.95	152	4.67	5.87	3.2	2.18	4.3	77
Er	2.06	1.39	1.8	0.9	2.96	135	2.43	3.05	1.56	0.94	2.64	247	9.35	19.2	5.44	3.06	9.8	118
Yb	2.39	1.51	2.17	1.18	3.2	546	2.54	3.82	1.7	0.92	2.75	652	9.56	14.8	7.7	4.62	11.57	687
Lu	0.36	0.24	0.32	0.17	0.5	447	0.36	0.53	0.23	0.12	0.38	494	1.37	1.97	1.07	0.68	1.6	488
Y	21.2	13.7	19	11	28	845	24	21.3	21	14	30	918	98.2	93	79	45	120	1217

Note: X is the mean; S is the standard deviation; M is the median; Q_L is the lower quartile; Q_H is the upper quartile; and n is the set volume. Concentrations of major elements are in wt %, and trace elements are in ppm.

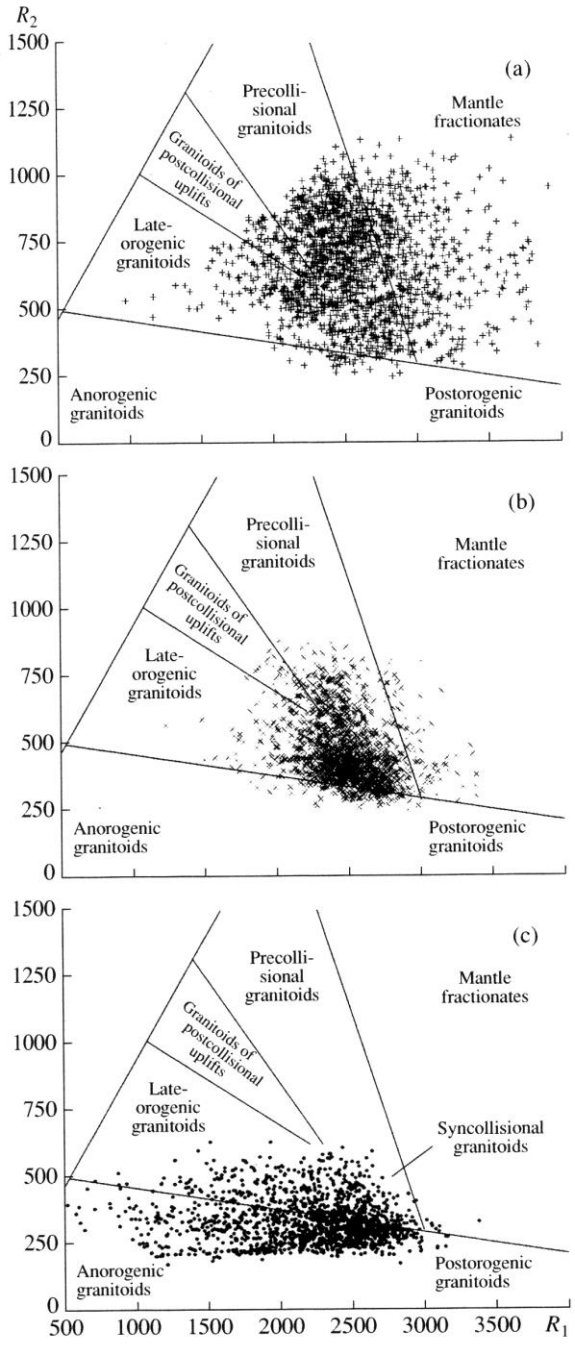

Fig. 2. Discriminant diagram R_1–R_2 (Batchellor and Bowden, 1985) with the points of (a) subduction, (b) collisional, and (c) within-plate granitoids. Here and in Figs. 3, 4, 5, 8, and 9, the points, oblique crosses, and crosses show the compositions of within-plate, collisional, and subduction granitoids, respectively. $R_1 = 4SiO_2 - 11(Na_2O + K_2O) - 2(FeO + TiO_2)$ and $R_2 = 6CaO + 2MgO + Al_2O_3$, mole fractions.

same degree by diverse analytical data obtained in a number of laboratories, which most likely excludes the presence of systematic between-group errors. On the other hand, the correctness of determination may vary considerably and its numeric estimation is impossible. In such a case, the only criterion for the validity of the use of available analytical data is that the natural dispersion of trace element contents in the granitoid groups considered must be higher than the respective analytical uncertainties. As will be shown below, according to the available analytical data, the granitoids of the geodynamic settings considered are significantly different in most trace elements (Table 2; Figs. 6, 7), and their use for discriminant analysis significantly reduces the empirical risk of improper classification (Table 3). Thus, it can be supposed with much confidence that the above criterion is held in our case.

The concentrations of most rock-forming elements in the granitoids are adequately approximated by the normal distribution. Because of this, the results of silicate analyses were preliminary screened rejecting values lying outside $X \pm 3S$, where X is the mean and S is the standard deviation. The rejection of outliers was not carried out for trace elements, which often show more complex distributions.

PREVIOUS WORK

The compiled analytical data set was first used for the assessment of the discriminating power of methods proposed by various authors to determine the tectonic position of granitoids from their chemical compositions.

One of the earliest attempts at discriminating granitoids from various settings on the basis of their chemical characteristics was the diagram of Batchellor and Bowden (1985) in the coordinates of petrochemical parameters R_1 and R_2, which were previously used for the classification of silicic igneous rocks (de la Roch *et al.*, 1980). The position of subduction, collisional, and within-plate granitoids on this diagram is shown in Fig. 2. The distribution of granitoid points on this diagram is in general consistency with the distinguished fields: the maxima of distribution of points of subduction, collisional, and within-plate granitoids fall within the appropriate fields. However, there are considerable variations exceeding the limits of fields on this diagram, and the compositions of subduction, collisional, and within-plate granitoids overlap in part, which suggests a low discriminating power of this diagram. It reflects only the most general features of the differences between the chemical compositions of granitoids.

Papu *et al.* (1989) proposed a set of simple petrochemical diagrams for the tectonic classification of granitoids. However, these diagrams were constructed on the basis of a small (less than 500 analyses) and not quite representative data set. In particular, their

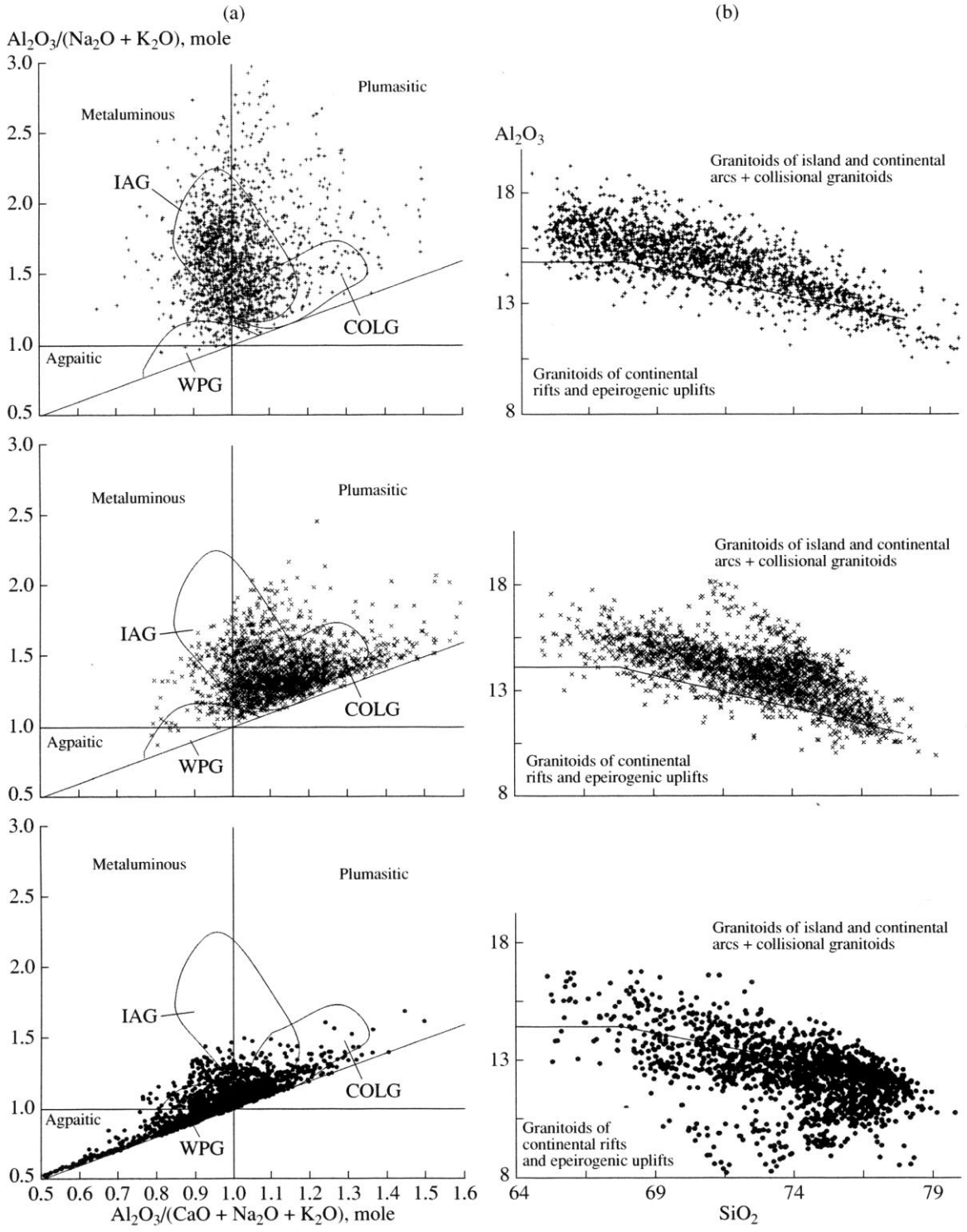

Fig. 3. Examples of discriminant diagrams, (a) SiO_2–Al_2O_3 (wt %) and (b) A/CNK–A/NK (Papu *et al.*, 1989) with the points of within-plate (lower diagram), collisional (middle diagram), and subduction (upper diagram) granitoids. Here (Fig. 3a) and in Figs. 4–12: WPG, COLG, and IAG are the within-plate, collisional, and island-arc (subduction) granitoids, respectively.

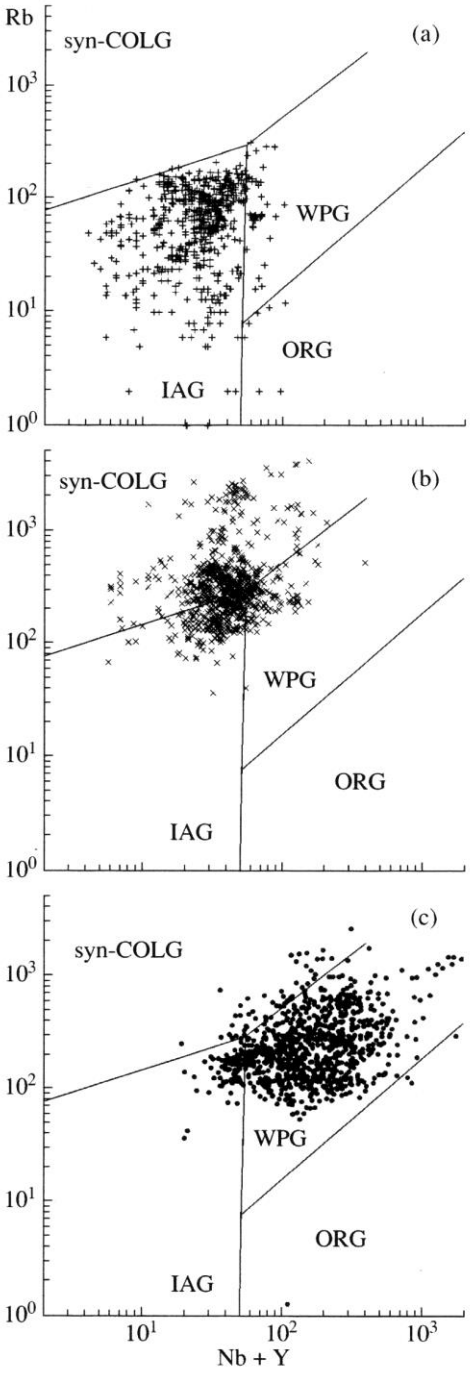

Fig. 4. Discriminant diagram (Y + Nb)–Rb (Pearce *et al.*, 1984) with the points of (a) subduction, (b) collisional, and (c) within-plate granitoids. ORG denotes oceanic ridge granitoids, and other abbreviations are the same as in Fig. 3.

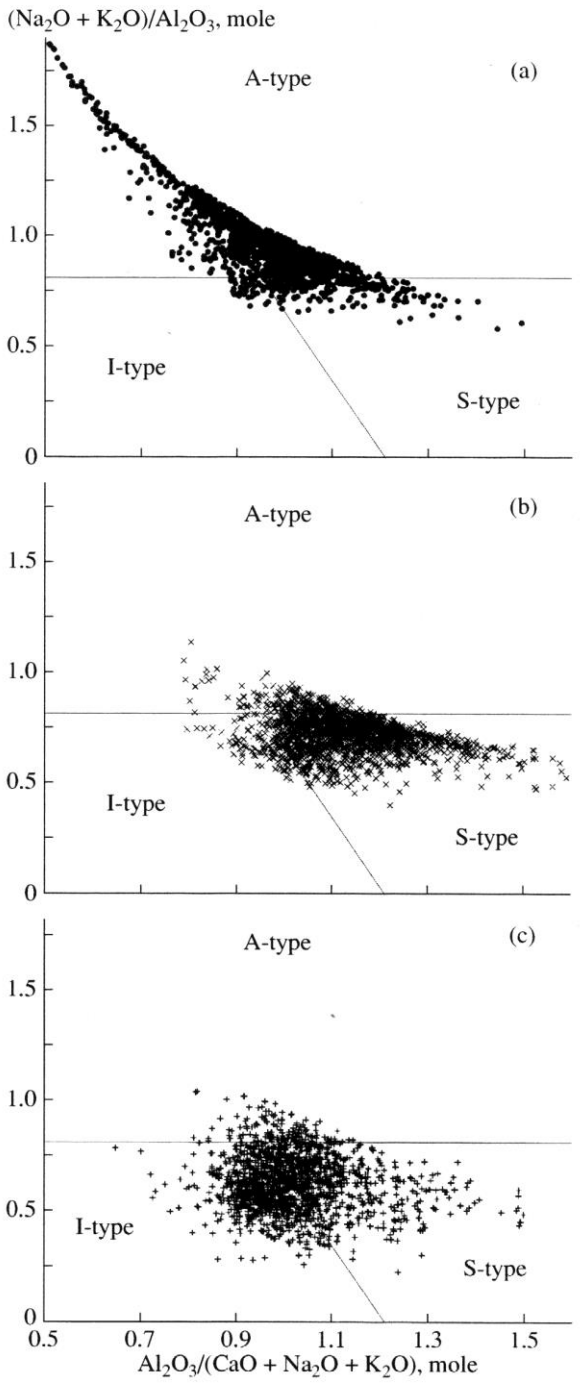

Fig. 5. Discriminant diagram A/(C + N + K)–(N + K)/A (Maeda, 1990) with the points of (a) subduction, (b) collisional, and (c) within-plate granitoids.

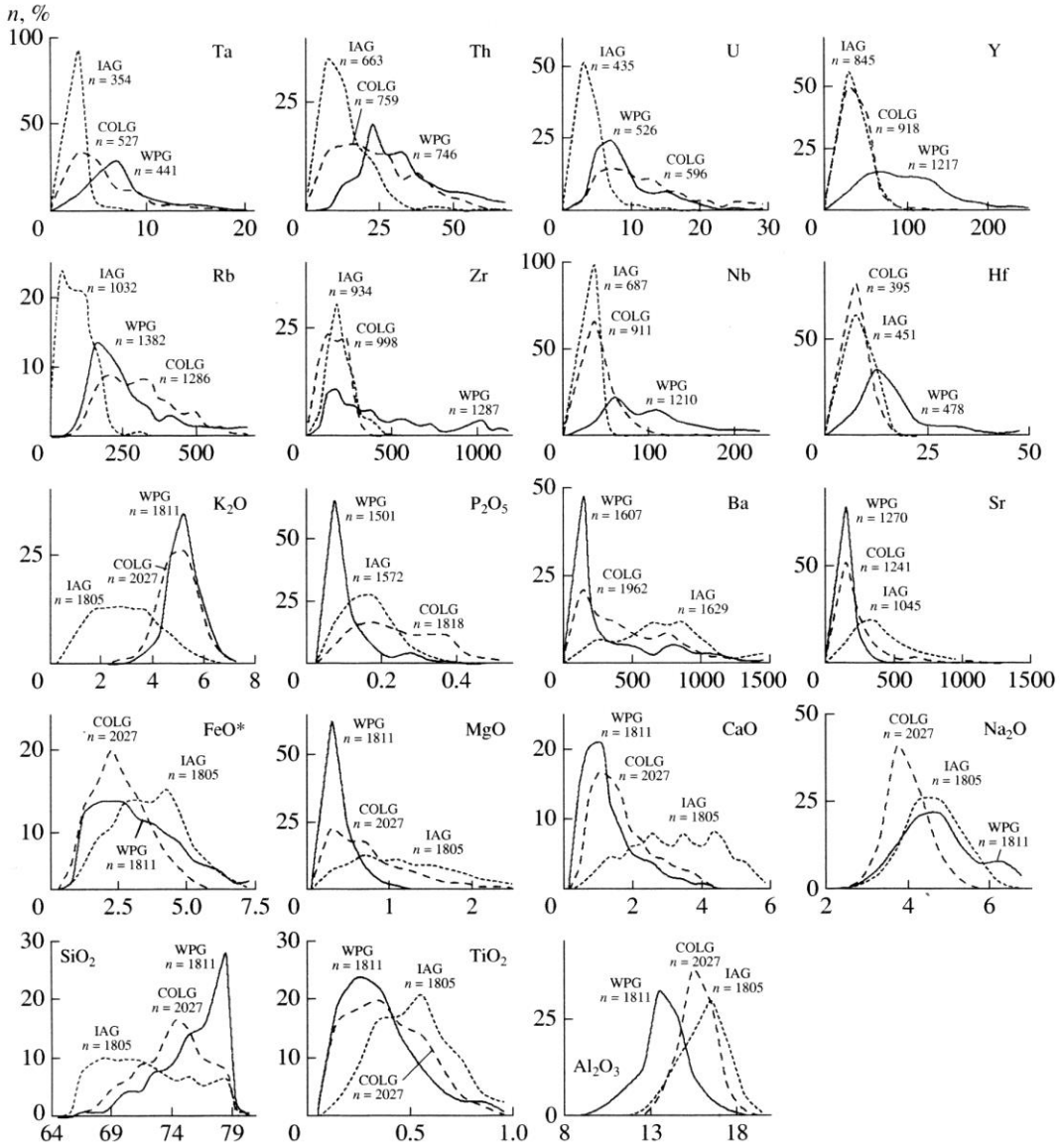

Fig. 6. Distribution of concentrations of major (wt %) and trace (ppm) elements in subduction, collisional, and within-plate granitoids. *n*, % is the volume of the data set.

reference island-arc granites included only the data on the complexes of Papua, New Guinea, and the Solomon Islands; continental margin granitoids were represented by data from the Sierra Nevada batholith only; collision granitoids, by the Himalayan granitoids and the Idaho batholith; and within-plate granitoids, by the igneous rocks of the Oslo rift and granitoid complexes of Nigeria. In this paper we cannot present the results of the test of all diagrams proposed by Papu *et al.* (1989). Only two of them are shown in Figs. 3a and 3b. Similarly to the previous case, the distribution of data points suggests that these diagrams have an inadequate discriminating power and reflect only the most general features of chemical differences between the granitoids considered. The practical application of this method may result in serious errors.

The most universally accepted geochemical method for the determination of the tectonic position of granitoids is currently the diagram of Pearce *et al.* (1984). This diagram is also based on a relatively small number of initial data, about 650 analyses. The concentrations of only three informative elements, Rb and (Y + Nb),

are used as discriminating factors. The diagram was constructed for the discrimination between oceanic, island-arc, within-plate, and syncollisional granitoids. Its significant drawback is that it does not allow recognition of late-collisional granites, which compose a considerable portion of collision magmatism. This diagram is more efficient than the series of diagrams proposed by Papu *et al.* In particular, the points of within-plate and subduction granitoids occur in the respective fields (Fig. 4). However, the compositions of island-arc and collisional granitoids show a considerable overlap, which significantly decreases the possibility of their correct classification. It should be noted that Fig. 4 displays the points of both syncollisional and late-collisional granitoids. However, the addition of data on late-collisional granitoids does not increase the extent of the compositional overlap of syncollisional and island-arc granitoids.

The systematics of granitoids on the basis of their hypothetical sources was proposed by Chappel and White (1974) and Whalen *et al.* (1987) and is now universally accepted. This classification is also widely used in tectonic reconstructions. It was suggested that I-granites are formed in subduction settings; S-granites, in collision settings; and A-granites, in within-plate settings. The logic of such an approach is probably in general correct, but the degree of correspondence has never been rigorously assessed. Maeda (1990) proposed the A/CNK–(N + K)/A diagram for the petrochemical classification of A-, S-, and I-granites. This diagram adequately assigns the reference samples of A-, S-, and I-granites. The majority of points of within-plate granitoids occur in the field of A-granites; collisional granitoids, in the field of S-granites; and island-arc granitoids, in the fields of S- and I- granites (Fig. 5). The maximum of the distribution of island-arc granitoid points corresponds to the line dividing the fields of S- and I-granites. Thus, the diagram reveals the correlation of within-plate granitoids with A-type anorogenic granites and, similarly to the previous case, allows their reliable classification. However, the use of this diagram for the classification of collisional and subduction granitoids may lead to significant errors, because the latter are not correlated with the I-type only. A surprising correlation between subduction granitoids and S- and I-types should be also noted. It would be more understandable if the points of collisional granitoids occurred in the fields of S- and I-granitoids, because their source was evidently heterogeneous and involved sedimentary rocks and previous precollisional (mainly, subduction) granitoids. It is possible that the heterogeneity of the source of subduction granitoids was controlled by the processes of contamination of crustal material.

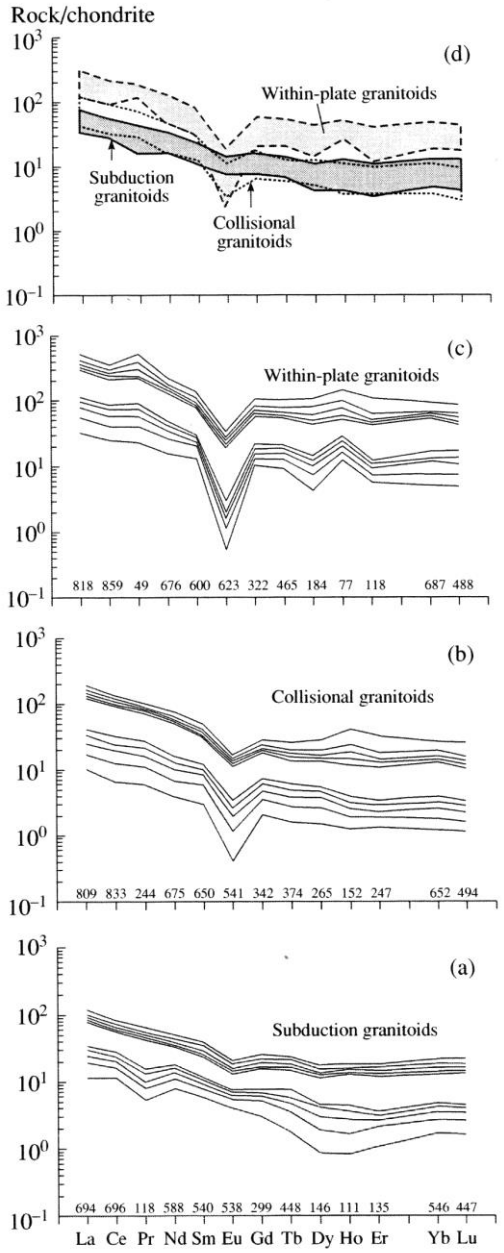

Fig. 7. Distribution of chondrite-normalized REE contents in granitoids of (a) subduction, (b) within-plate, and (c) collisional environments. The outer contour in Figs. 7a–7c envelopes 90% of analytical data, and the inner contour, 50% (isolines of distribution are drawn through 10%). Numerals above the *x* axis are the total numbers of analyses. Figure 7d shows the non-parametric estimate of REE contents within the lower and upper quartiles.

Table 3. Coefficients of discriminant functions, $D(x)$ separating granitoids of the major geodynamic settings using the concentrations of major and trace elements

Component	1	2	3	4	5	6	7	8	9	10	11	12	13
	IAG – WPG		COLG – WPG			IAG – COLG						IAG – (COLG + WPG)	
	$F_{(i-w)1}$	$F_{(i-w)2}$	$F_{(c-w)1}$	$F_{(c-w)2}$	$F_{(c-w)3}$	$F_{(i-c)1}$	$F_{(i-c)2}$	$F_{(i-c)3}$	$F_{(i-c)4}$	$F_{(i-c)5}$	$F_{(i-c)6}$	$F_{(i-wc)1}$	$F_{(i-wc)2}$
SiO_2	869.06	387.94	−3813.7	−752.30	−1099.79	2415.26	1853.76	1208.41	1267.96	1098.93	651.80	2432.42	845.93
TiO_2	3858.13	2199.22	−9848.82	−6537.06	−3804.50	5551.06	5007.73	3502.82	3197.92	2629.87	1318.50	7900.33	3847.0
Al_2O_3	1390.98	573.53	−2946.6	−25.60	−736.91	2013.29	1663.92	1162.97	1030.99	975.58	659.95	2512.12	872.66
FeO	144.39	215.85	−3971.19	−928.96	−1094.93	2089.48	1589.96	1077.25	1154.08	1024.87	681.40	1380.23	576.69
MgO	2103.63	488.07	−849.14	1928.07	−60.14	1910.27	1565.28	716.03	856.75	722.54	348.39	2616.55	465.61
CaO	1514.13	458.77	−3430.32	−464.21	−962.82	3515.13	2712.67	1676.87	1803.99	1527.55	777.96	3480.51	1067.69
Na_2O	554.80	206.53	−5082.39	−1808.19	−1665.50	3997.33	3253.66	2098.58	2273.31	2037.37	954.89	3045.39	1005.42
K_2O	−1033.07	−308.29	−4325.89	−1272.16	−1117.29	1216.88	768.77	461.78	415.49	256.99	163.42	645.91	137.96
P_2O_5	–	–	–	8675.33	–	–	−4840.1	–	–	–	–	–	–
Rb	–	–	–	–	–	–	–	−1.23	–	−0.69	−1.29	–	–
Ba	–	–	–	–	–	–	–	–	1.42	1.30	0.66	–	–
Sr	–	–	–	–	–	–	–	–	−0.21	−0.42	−0.59	–	–
La	–	−0.05	–	–	−0.96	–	–	–	–	–	–	–	3.74
Ce	–	−0.89	–	–	0.59	–	–	–	–	–	−5.16	–	−1.22
Nd	–	−3.87	–	–	−4.26	–	–	–	–	–	−1.30	–	−12.96
Sm	–	–	–	–	–	–	–	–	–	–	18.53	–	–
C	−86675.5	−38030	376358.7	71073.5	107445.6	−239088	−184920	−121363	−125716	−109768	−64665	−241285.5	−83008.2
D^2	2.79	2.78	2.24	2.39	2.38	2.36	2.46	2.45	2.62	2.63	2.76	2.56	2.68
R, %	7.02	5.77	9.8	9.66	8.7	12.2	11.5	10.3	9.2	9.0	7.5	10.4	8.6
n_1	1805	576	2027	1818	646	1805	1572	1032	949	921	423	1805	576
n_2	1811	636	1811	1504	636	2027	1818	1249	1119	1075	554	3838	1282

Note: (1)–(2) Discriminant functions dividing granitoids of subduction (IAG) and within-plate (WPG) environments; (3)–(8) discriminant functions dividing granitoids of collisional (COLG) and within-plate (WPG) environments; (6)–(11) discriminant functions dividing granitoids of subduction (IAG) and collisional (COLG) environments; and (12)–(13) discriminant functions dividing granitoids of subduction (IAG) and combined within-plate and collisional (WPG + COLG) environments. The discriminant functions have the form $D(x) = \Sigma a_i x_i + C$, where $a_i x_i$ is the product of the coefficient of the discriminant function and the concentration of the respective element and C is the discriminant threshold. If $D(x) > 0$, the object classified belongs to the first set. The concentrations of major elements were recalculated to a water-free basis. The concentrations of major elements are in wt %, and trace elements are in ppm. D_2 is the generalized Mahalanobis distance, R is the empirical risk of incorrect classification, and n_1 and n_2 are the volumes of the sets compared.

GEOCHEMICAL CHARACTERISTICS OF GRANITOIDS FROM MAJOR GEODYNAMIC ENVIRONMENTS

The generalized statistical characteristics of the chemical composition of granitoids from the geodynamic environments considered are listed in Table 2, and the distribution of the concentrations of chemical elements are shown in Fig. 6. The chondrite-normalized REE distribution patterns are shown in Fig. 7. The inspection of these data suggests that the three granitoid groups are statistically different in the concentrations of many chemical elements. The most significant differences were observed between within-plate and subduction granitoids. The characteristic features of the distribution of most chemical elements allow us to consider these granitoids as two polar groups, whereas collisional granitoids usually show transitional compositions. This is most clearly seen in the SiO_2 distribution: subduction granitoids show an almost uniform SiO_2 distribution with a broad maximum near 69%, within-plate granitoids show a nonsymmetrical left-sided distribution with a sharp maximum near 78%, and collisional granitoids show a relatively symmetrical distribution with a maximum at 75%. Collisional granitoids resemble the granitoids of within-plate environments with respect to contents of most major elements (except for Na and P) and some trace elements (Sr, Rb, Th, U, and Eu) and approach the granites of subduction environments with respect to the character of La, Ce, Nd, Sm, Gd, Ho, Tb, Er, Yb, Y, Zr, Nb, and Hf distribution (Fig. 6, Table 2).

Although the granitoids of the geodynamic settings considered differ significantly in the contents of many chemical elements, the applicability of these data for their geochemical classification is in general limited because of the wide overlap of the distributions of particular elements. However, the established differences imply that reliable and efficient discrimination criteria can be obtained by means of multidimensional statistical analysis.

CLASSIFICATION OF SUBDUCTION, COLLISIONAL, AND WITHIN-PLATE GRANITOIDS BY MEANS OF LINEAR DISCRIMINANT FUNCTIONS

The granitoid groups were separated using the apparatus of discriminant functions. For this purpose we used a variant of discriminant analysis described by Rodionov *et al.* (1987, pp. 154–156), which assumes inequality of the covariance matrices of the sets compared and includes estimation of distribution parameters from a set. This variant yields two solutions, linear and quadratic discriminant functions. In our case, the quadratic discriminant functions appeared to be less informative and are not considered in this paper.

The examination of the geochemical methods that have been proposed for the classification of granitoids of various geodynamic settings demonstrated that they are rather reliable for the granitoids of within-plate settings and granitoids of compression regimes (subduction and collisional) (Figs. 4, 5). Because of this, an important improvement of available methods would be the separation of subduction and collisional granitoids.

This problem can be solved by discriminant analysis. Table 3 presents a number of discriminant functions, which adequately separate subduction and collisional granitoids and are ranked with respect to decreasing empirical risk of incorrect classification (nos. 6–12). These functions provide a significant improvement in the efficiency of geochemical classification methods for granitoid from various geodynamic settings. For instance, it is possible to construct discrimination diagrams on the basis of combinations of the calculated discriminant functions and some parameters of previously proposed diagrams. In particular, the parameter (N + K)/A or (Y + Nb) can be plotted along one axis, which provides a reliable separation of within-plate granitoids from the combined set of island-arc and collisional granitoids (Figs. 4 and 5, respectively), and one of the discriminant functions on the other axis (Table 3, nos. 6–12).

On the other hand, there are various methods of recognition on the basis of the results of discriminant analysis shown in Table 3. For instance, granitoids of the geodynamic settings considered can be classified on the basis of petrochemical data only using the discriminant functions of Table 3 (nos. 1, 3, 6) and the scheme of dichotomous division. Using the function $F_{(i-w)1}$ (no. 1), the object studied can be assigned to subduction + collisional or within-plate + collisional granitoid groups. A further classification is made by the functions $F_{(c-w)1}$ (no. 3) and $F_{(i-c)1}$ (no. 6). More reliable results can be obtained using similar discriminant functions (Table 3) including the concentrations of the most commonly analyzed trace elements, which are characterized by smaller probability of incorrect classification (R): function no. 2 in the first stage and function nos. 4, 5, and 7–11 in the following stages of recognition.

Table 3 presents the optimum variants of discriminant functions dividing the sets of granitoids considered. In fact, the number of all possible discriminant functions is much greater. The choice of optimum variants took into account the interplay of two factors: small value of the risk of incorrect classification and representativeness of the data sets compared. In other words, the choice was dictated, on the one hand, by the use of the most informative chemical elements as arguments and, on the other hand, by the search for a combination of the chemical elements providing the representativeness of the data set. This scheme resulted in some cases in the elimination of rather informative but rarely analyzed elements from the set of arguments. The results of recognition on the basis of different discriminant functions from Table 3 are not identical but fairly similar. In this respect, each of them can be used

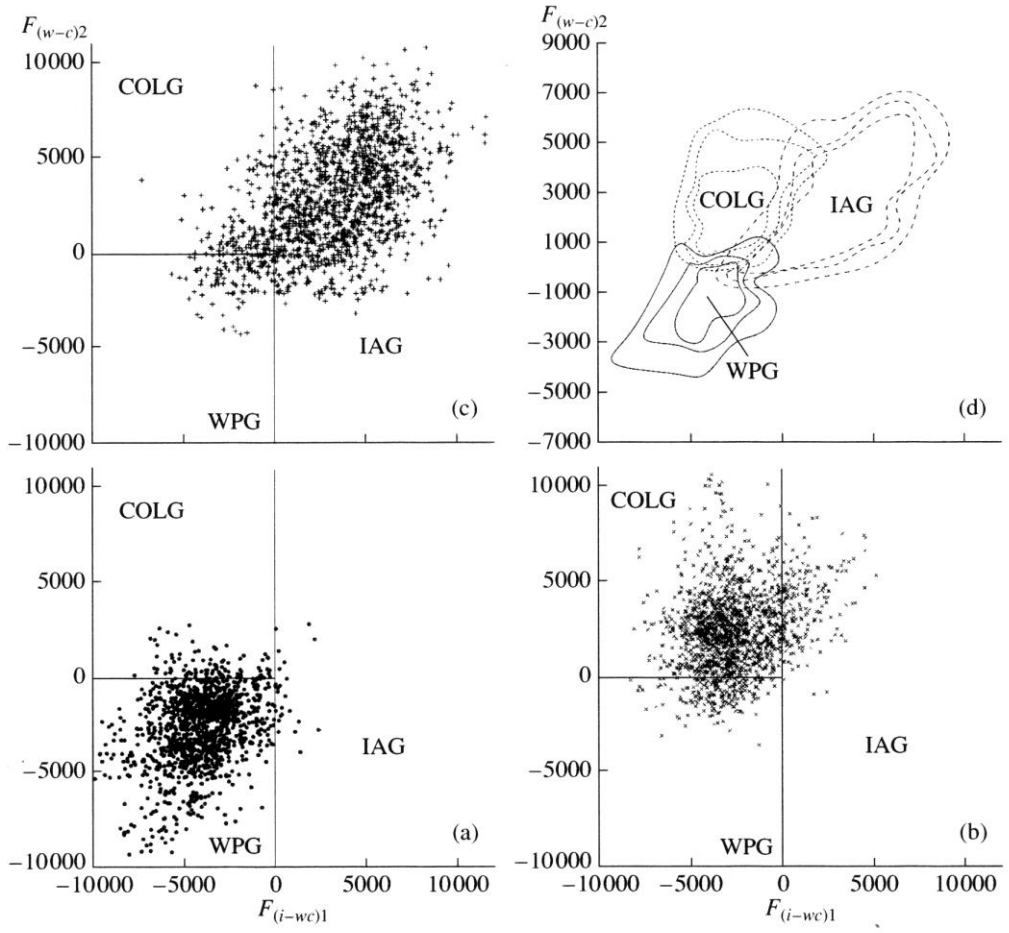

Fig. 8. Discrimination diagram $F_{(i-wc)1}$–$F_{(c-w)2}$ with the points of (a) within-plate, (b) collisional, and (c) subduction granitoids and (d) isolines of the density of distribution of the granitoid points considered. The outer contour envelopes 90% of the data points; middle contour, 80%; and the inner contour, 70%. The formulas for the calculation of the coordinates are given in Table 3.

in practice but, if the necessary analytical data are available, the functions with the lower risk of incorrect classification R are preferable.

One of the drawbacks of the above-described approach is that the results of recognition are difficult to present in a clear graphical form, because this implies the construction of three-dimensional diagrams. However, the graphical presentation of the results of recognition is desirable especially in the case of point occurrence near field boundaries, because it provides additional information for the choice of the most adequate solution. Two variants of the graphical recognition of the geodynamic setting of granitoid formation are considered below: (a) using only major elements and (b) using major and trace elements providing the minimum risk of incorrect classification. For this purpose we calculated additional discriminant functions, in particular, $F_{(i-wc)1}$ and $F_{(i-wc)2}$ (nos. 12–13), separating subduction granitoids from the combined set of collisional and within-plate rocks. For example, the binary diagram with $F_{(i-wc)1}$ on the abscissa and $F_{(c-w)1}$ (or $F_{(c-w)2}$) on the ordinate efficiently separates the granitoids of various geodynamic settings using the concentrations of major elements only.

The discriminant diagram $F_{(i-wc)1}$–$F_{(c-w)1}$ was published by Velikoslavinskii and Velikoslavinskii (2001), and $F_{(i-wc)1}$–$F_{(c-w)2}$ is shown in Fig. 8. Formally, discriminant analysis implies that the lines separating the fields of subduction, within-plate, and collisional granitoids must coincide with the coordinate axes. However, the character of the distribution of granitoid points (Figs. 8a–8c) and results of their statistical analysis (Fig. 8d) suggest that the coordinate axes approximate adequately only the boundaries of the within-plate granitoid field, whereas the dividing line between the fields of subduction and collisional granitoids does not coincide with the coordinate axis.

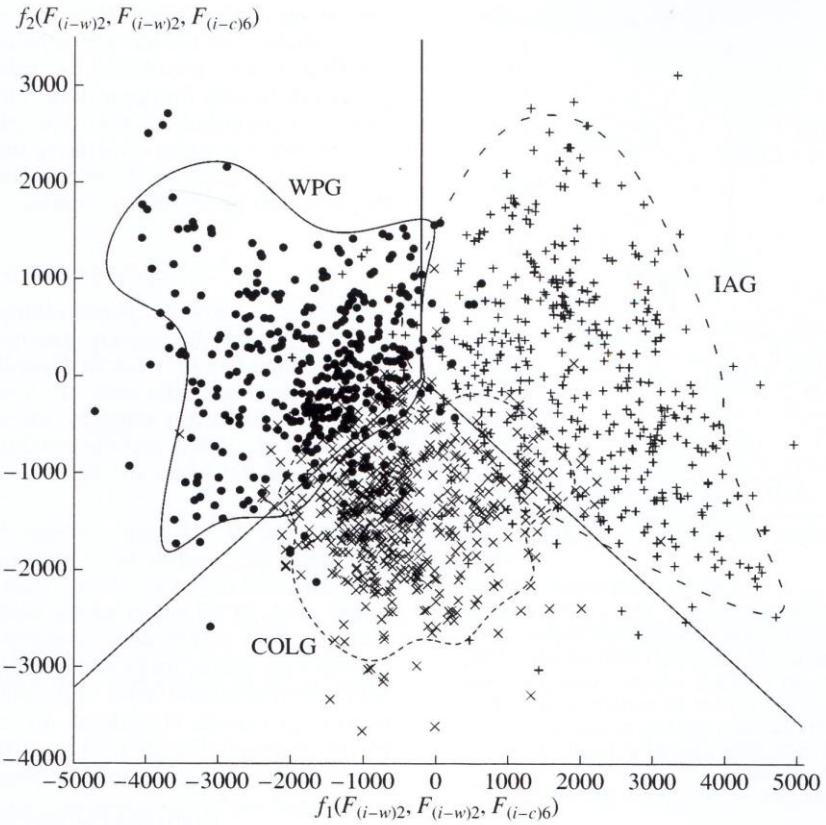

Fig. 9. Discriminant diagram $f_1(F_{(i-w)2}, F_{(c-w)3}, F_{(i-c)6})$–$f_2(F_{(i-w)2}, F_{(c-w)3}, F_{(i-c)6})$ with the points of within-plate, collisional, and subduction granitoids. The contours comprise 95% distributions of the data points. $f_1(F_{(i-w)2}, F_{(c-w)3}, F_{(i-c)6}) = 196.203SiO_2 + 753.953TiO_2 + 481.96Al_2O_3 + 92.664FeO^* + 521.5MgO + 374.766CaO + 7.571Na_2O - 584.778K_2O + 0.379Ba - 0.339Sr - 0.733Rb - 0.429La - 3.33Ce - 5.242Nd + 10.565Sm - 19823.8$ and $f_2(F_{(i-w)2}, F_{(c-w)3}, F_{(i-c)6}) = 1292.962SiO_2 + 4002.667TiO_2 + 1002.231Al_2O_3 + 1297.136FeO^* + 262.067MgO + 1250.48CaO + 1923.417Na_2O + 1009.287K_2O + 0.3634Ba - 0.325Sr - 0.701Rb + 0.8015La + 3.347Ce + 2.68Nd + 10.11Sm - 126860.0$.

The comparison of the empirical errors of classification of the discriminant functions used for the construction of discriminant diagram (Fig. 8) with the empirical errors of functions with concentrations of major and trace elements as arguments shows that the $F_{(i-wc)1}$–$F_{(c-w)2}$ diagram is attractive, because it allows estimation of the tectonic position of granitoids using the results of silicate analysis only, but not optimal with respect to the risk of incorrect classification. Because of this, we constructed a discriminant diagram in the coordinates that minimize the value of this error.

In particular, such coordinates can be represented by the discriminant functions $F_{(i-w)2}$, $F_{(c-w)3}$, and $F_{(i-c)6}$ (Table 3, nos. 2, 5, and 11), whose arguments include major and trace elements. As was shown above, these functions allow recognition in an analytical form, whereas graphical presentation requires the construction of a three-dimensional diagram. A discriminant function was calculated separating subduction granitoids from the combined set of within-plate and collisional granitoids using the contents of major elements and providing the minimum classification error. This function is given in column 13 in Table 3. However, the error of classification of the function $F_{(i-wc)2}$ (8.6%) is significantly higher than the errors of classification of the functions discriminating subduction and collisional (7.5%) and subduction and within-plate (5.8%) granitoids separately. Therefore, the use of this discriminant function as a coordinate axis is irrational. In order to transform the discrimination diagram $F_{(i-w)2}$–$F_{(c-w)3}$–$F_{(i-c)6}$ into a two-dimensional form, the following procedure was applied. The values of the discriminant functions $F_{(i-w)2}$, $F_{(c-w)3}$, and $F_{(i-c)6}$ calculated for island-arc, collisional, and within-plate granitoids were processed by principal component analysis (calculation from the covariance matrix). The principal components were obtained with loadings of 70.18, 28.15, and 1.67%. Thus, there is an opportunity to construct a discriminant diagram without a significant loss of information using the first and second principal components. The first and second principal components are calcu-

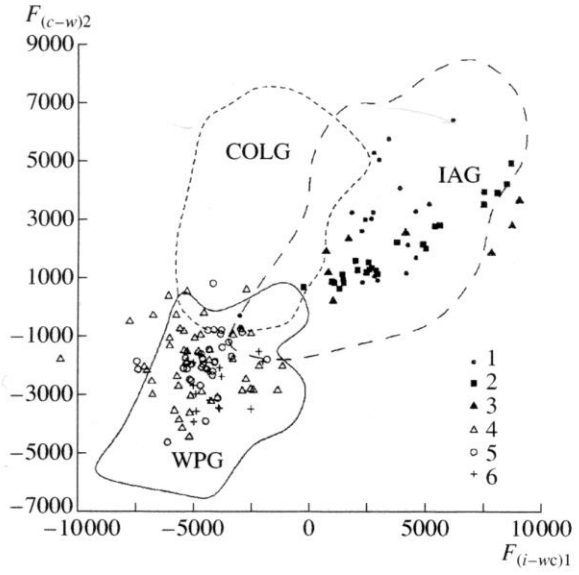

Fig. 10. Discriminant diagram $F_{(i-wc)1}$–$F_{(c-w)2}$ with the points of Precambrian subduction and within-plate granitoids. (1)–(3) Subduction granitoids: (1) Norseman-Wiluna belt, (2) Birbir arc, and (3) Idsas; (4)–(6) within-plate granitoids: (4) igneous complexes of the northern Baikal volcanoplutonic belt, (5) Ragunda rapakivi massif, and (6) rift-related granitoids of the Robertson River basin. Other symbols are the same as in Fig. 8.

lated by the formulas: $f_1(F_{(i-w)2}, F_{(c-w)3}, F_{(i-c)6}) = 0.711F_{(i-w)2} + 0.411F_{(c-w)3} + 0.57F_{(i-c)6}$ and $f_2(F_{(i-w)2}, F_{(c-w)3}, F_{(i-c)6}) = 0.05F_{(i-w)2} - 0.837F_{(c-w)3} + 0.545F_{(i-c)6}$.

Figure 9 shows the diagram $f_1(F_{(i-w)2}, F_{(c-w)3}, F_{(i-c)6})$ versus $f_2(F_{(i-w)2}, F_{(c-w)3}, F_{(i-c)6})$ with the points of granitoids of the environments considered and 95% contours of the compositional fields. Its coordinates were transformed into a form convenient for calculations by substituting $F_{(i-w)2}$, $F_{(c-w)3}$, and $F_{(i-c)6}$ values from Table 3 into the above formulas.

In addition, we attempted to perform a more detailed geochemical discrimination of each granitoids group (subduction, collisional, and within-plate) into subgroups in accordance with the classification presented in Table 1. However, no significant differences were found between the subgroups of granitoids. The problem of a more detailed tectonic classification of granitoids probably requires further special investigations.

TESTING OF THE METHOD ON THE EXAMPLE OF PRECAMBRIAN GRANITOIDS

The proposed geochemical methods of the geotectonic classification of granitoids may be helpful in the tectonic reconstructions of various regions. Their application is probably most promising in the tectonic analysis of Precambrian complexes, where other criteria may be less informative. However, since these criteria were obtained on the basis of geochemical data mainly for Phanerozoic granitoids, the validity of the use of geochemical data for the tectonic classification of Precambrian granitoids is not quite obvious. Below we give several examples illustrating the possibility of the tectonic classification of Precambrian granitoids using the proposed geochemical criteria.

Subduction Granites

Subduction granitoids are exemplified by the Late Archean continental-margin granitoids of the Norseman–Wiluna belt of Western Australia (Cassidy *et al.*, 1991), the Late Precambrian tonalite–trondhjemite complex of the Birbir magmatic arc of western Ethiopia (Wolde *et al.*, 1996), and the trondhjemite–granophyre complex of the Idsas arc of Saudi Arabia (Al-Shanti *et al.*, 1984).

Eighteen of 20 points of the Norseman–Wiluna granitoids plot within the subduction granitoid field (Fig. 10), and only two points occur within the uncertainty field; of 25 points of the Idsas granitoids, only one point falls within the uncertainty field; and all eight points of the Birbir arc granitoids are located within the subduction granitoid field. Thus, the examples of subduction granitoids considered are correctly classified by the proposed discriminant functions.

Collisional Granitoids

One of the examples of Precambrian granitoids are the late kinematic microcline granites of the northern Ladoga region (Putsarskii, Borodinskii, Zavetinskii, Kuznechinskii, and Tervusskii plutons), which form a linear northeast-striking zone about 100 km long with an age of ~1.8 Ga and were probably related to the collision of the Ladoga block and the Karelian craton (Shinkarev and Grigor'eva, 1995; Velikoslavinskii, 1999; etc.). Figure 11 shows the distribution of 179 points of the microcline granites of the northern Ladoga region (Velikoslavinskii, 1999). About 73% of these points correspond unambiguously to collision granitoids; 10% lie in the uncertainty fields; and 17%, in the fields of within-plate and island-arc granitoids.

Also shown in Fig. 11 are the points of the Early Proterozoic (~2 Ga) granites of the Transamazonian orogen (Cuney *et al.*, 1990), which owed its formation to a continental collision. Although three of 11 point of these granites occur in the uncertainty field, the granites are unequivocally classified as collisional rocks. The consideration of trace elements results in a more reliable classification: all data points are located within the field of collisional granitoids (Fig. 12).

Within-Plate Granitoids

Within-plate Precambrian magmatism is exemplified by (1) within-plate igneous rocks of the northern

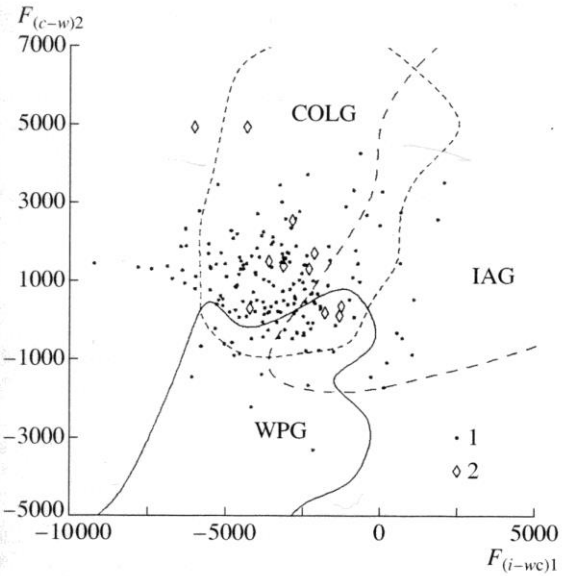

Fig. 11. Discriminant diagram $F_{(i-wc)1}$–$F_{(c-w)2}$ with the points of Precambrian collisional granitoids. (1) Microcline granites of the northern Ladoga region and (2) granites of the Transamazonian orogen. Other symbols are the same as in Fig. 8.

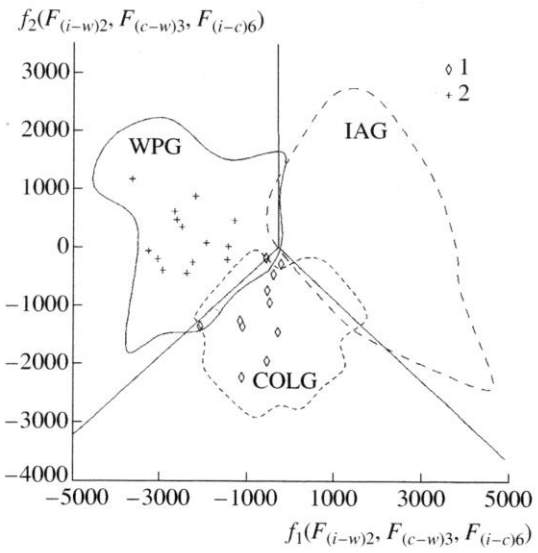

Fig. 12. Discriminant diagram $f_1(F_{(i-w)2}, F_{(c-w)3}, F_{(i-c)6})$–$f_2(F_{(i-w)2}, F_{(c-w)3}, F_{(i-c)6})$ with the points of (1) Precambrian collisional granitoids of the Transamazonian orogen and (2) within-plate rift granitoids of the Robertson River basin.

Baikal volcanoplutonic belt (extrusive rocks of the Akitkanskaya Group and granitoids of the Irelskii and Primorskii complexes) with an age of 1.82–1.87 Ga, which were characterized by Salop (1967), Manuilova *et al.* (1964), and Neimark *et al.* (1998); (2) rapakivi granites of the Ragunda complex (Kornfält, 1976); and (3) Late Precambrian (702–735 Ma) extrusive rocks and granitoids of the Robertson River basin of the Blue Ridge Province, Virginia related to the early stages of Laurentian rifting (Tollo and Aleinikoff, 1996).

Only three of 48 points of the rocks of the northern Baikal volcanoplutonic belt (Fig. 10) fall beyond the field of within-plate granitoids (one point lies in the field of collision granitoids and two points, in the uncertainty field). Four of the 35 points of the granites of the Ragunda complex (Fig. 12) are located outside the field of within-plate granitoids (one point in the field of collision granitoids and three points in the uncertainty field). All the points of the rift-related granitoids of the Robertson River basin (Figs. 10, 12) are located within the field of within-plate granitoids. Overall, the examples of within-plate granitoids considered are reliably classified as within-plate granitoids in the proposed discriminant diagram.

Thus, the examples considered suggest the validity of the proposed discriminant functions for the tectonic analysis of Precambrian granitoids.

CONCLUSIONS

The following results were obtained in our study:

(1) The statement on the geochemical individuality of granitoids from within-plate, subduction, and collisional environments was corroborated.

(2) A generalized geochemical portrait was provided for the granitoids of the geodynamic environments considered.

(3) The methods that are commonly used for the determination of the geodynamic environment of granitoid formation on the basis of chemical characteristics were revised. It was demonstrated that their application may lead to erroneous results.

(4) Discriminant functions were calculated for the more reliable solution of the problem of the tectonic classification of granitoids of primary igneous nature (volcanics of dacite–rhyolite composition and intrusive granodiorites and granites with $SiO_2 > 65$ wt %). The systematics shown in Figs. 8d and 9 are of special interest for practical application. The former allows the determination of granitoid formation setting from the results of silicate analysis only, and the latter is characterized by the lower error of incorrect classification but requires a wider spectrum of analytical data. If there is no analytical data for P_2O_5, the $F_{(i-wc)1}$–$F_{(c-w)1}$ diagram can be used (Velikoslavinskii and Velikoslavinskii, 2001, Fig. 4).

(5) The results of testing of the calculated discriminant functions on the example of Precambrian granitoids sug-

gest that the proposed method can be used for the tectonic reconstructions of Precambrian domains.

It should be taken into account that, although the proposed systematics allow one to reconstruct more reliably the geodynamic setting of granitoid formation, it does not solve all the problems of their tectonic classification. First, the fields of granitoids of the environments considered overlap in part, which may results in the occurrence of granitoids studied in uncertainty fields. Second, the proposed systematics ignored at least two widespread groups of granitoids: (1) intrusive granitoids formed under conditions of postcollisional extension and (2) diverse polygenetic ultrametamorphic granitoids. Their tectonic classification on the basis of geochemical data is a subject for future investigations.

ACKNOWLEDGMENTS

The author is particularly grateful to A.B. Kotov, V.A. Rudnik (Institute of Precambrian Geology and Geochronology, Russian Academy of Sciences), and E.V. Tolmacheva (All-Russia Institute of Geology) for helpful comments and suggestion during the preparation of the manuscript.

REFERENCES

Al-Shanti, A.M.S., Abdel-Monen, A.A., and Marzouki, F.H., Geochemistry, Petrology, and Rb–Sr Dating of Trondhjemite and Granophyre Associated with Jabal Tuys Ophiolite, Idsas Area, Saudi Arabia, *Precambrian Res.*, 1984, no. 3/4, pp. 321–334.

Batchellor, R.A. and Bowden, P., Petrogenetic Interpretation of Granitoid Rock Series Using Multicationic Parameters, *Chem. Geol.*, 1985, vol. 48, no. 1/4, pp. 43–55.

Chappel, B.W. and White, A.J.R., Two Contrasting Granite Types, *Pacific Geol.*, 1974, vol. 8, pp. 173–174.

Cuney, M., Sabate, P., Vidal, Ph., *et al.*, The 2 Ga Peraluminous Magmatism of the Jacobina–Contendas Mirante Belt (Bahia, Brazil): Major and Trace Element Geochemistry and Metallogenic Potential, *J. Volcanol. Geotherm. Res.*, 1990, vol. 44, pp. 123–141.

De La Roch, H., Leterrier, J., Grandclaude, P., and Marchal, M., A Classification of Volcanic and Plutonic Rocks Using the R1R2-Diagram and Major Element Analyses—Its Relationships with Current Nomenclature, *Chem. Geol.*, 1980, vol. 29, no. 3/4, pp. 183–210.

Förster, H.-J., Tischendorf, G., and Trumbull, R.B., An Evaluation of the Rb vs. (Y + Nb) Discrimination Diagram to Infertectonic Setting of Siliceous Igneous Rocks, *Lithos*, 1997, vol. 40, no. 4, pp. 281–293.

Kornfält, K.-A., Petrology of the Ragunda Rapakivi Massif, Central Sweden, *Sveriges Geologiska Undersökning*, 1976, Series C NR 725, vol. 70, no. 7, pp. 1–111.

Maeda, J., Opening of the Kuril Basin Deduced from the Magmatic History of Central Hokkaido, Northern Japan, *Tectonophysics*, 1990, vol. 174, no. 3/4, pp. 235–255.

Manuilova, M.M., Vas'kovskii, D.P., and Gurulev, S.A., *Geologiya dokembriya Severnogo Pribaikal'ya* (The Precambrian Geology of the Northern Baikal Area), Moscow–Leningrad: Nauka, 1964.

Neimark, L.A., Larin, A.M., Nemchin, A.A., *et al.*, Geochemical, Geochronological (U–Pb), and Isotopic (Pb, Nd) Evidences in Favor of Anorogenic Magmatism in the Northern Baikal Vulcano-Plutonic Belt, *Petrologiya*, 1998, vol. 6, no. 2, pp. 139–164.

Papu, D., Piccoli, M., and Piccoli, P., Tectonic Discrimination of Granitoids, *Bull. Geol. Soc. Am.*, 1989, vol. 101, pp. 635–643.

Pearce, J.A., Harris, N.B.W., and Tindle, A.G., Trace Element Discrimination Diagrams for the Interpretation of Granitic Rocks, *J. Petrol.*, 1984, vol. 25, no. 4, pp. 956–983.

Rodionov, D.A., Kugan, R.I., Golubeva, V.A., *et al.*, *Spravochnik po matematicheskim metodam v geologii* (Mathematical Methods in Geology: A Handbook), Moscow: Nedra, 1987.

Salop, L.I., *Geologiya Baikal'skoi gornoi oblasti* (The Geology of the Baikal Highland), Moscow: Nedra, 1967, vol. 2.

Shinkarev, N.F. and Grigor'eva, L.V., Granitoid Series of Collision Zones: Petrological and Geochemical Features and Genesis Problems, *Vestn. St. Peterb. Univ.*, 1995, ser. 7, no. 4, pp. 18–24.

Thiéblemont, D. and Cabanis, B., Utilization d'un diagramme (Rb/100)–Tb–Ta pour la discrimination geochimique et l'etude petrogenitique de roches magmatiques acides, *Bull. Geol. Fr.*, 1990, vol. 8, no. 1, pp. 23–35.

Tollo, R.P. and Aleinikoff, J.N., Petrology and U–Pb Geochronology of the Robertson River Igneous Suite, Blue Ridge Province, Virginia: Evidence for Multistage Magmatism Associated with an Early Episode of Laurentian Rifting, *Am. J. Sci.*, 1996, vol. 296, pp. 1049–1090.

Velikoslavinskii, D.A. and Velikoslavinskii, S.D., Microcline Granites of the Kartashev Pluton: Chemistry and Tectonic Position, *Zap. Vseross. Mineral. O-va*, 1999, part 130, no. 5, pp. 36–50.

Velikoslavinskii, D.A., The Origin of Porphyritic Microcline Granites of the Northern Ladoga Area and Karelia, *Zap. Vseross. Mineral. O-va*, 1999, part 128, no. 3, pp. 14–30.

Whalen, J.B., Currie, L.C., and Chappel, B.W., A-Type Granites: Geochemical Characteristics, Discrimination and Petrogenesis, *Contrib. Mineral. Petrol.*, 1987, vol. 95, no. 4, pp. 407–419.

Wolde, B. *et al.*, Tonalite–Trondhjemite–Granite Genesis by Partial Melting of Newly Underplated Basaltic Crust: An Example from the Neoproterozoic Birbir Magmatic Arc, Western Ethiopia, *Precambrian Res.*, 1996, vol. 76, no. 1/2, pp. 3–14.